

Molecular Dynamics Simulations Suggest that Electrostatic Funnel Directs Binding of Tamiflu to Influenza N1 Neuraminidases

Ly Le^{1,2,3,△}, Eric H. Lee^{1,4,5,△}, David J. Hardy¹, Thanh N. Truong², Klaus Schulten^{1,4,6,*}

1 Beckman Institute, University of Illinois at Urbana-Champaign, Urbana, USA.

2 Department of Chemistry, University of Utah, Salt Lake City, UT, USA.

3 School of Biotechnology, Ho Chi Minh International University and Saigon Institute for Computational Science and Technology, Ho Chi Minh City, Vietnam

4 Center for Biophysics and Computational Biology University of Illinois at Urbana-Champaign, Urbana, USA.

5 College of Medicine, University of Illinois at Urbana-Champaign, Urbana, USA.

6 Department of Physics, University of Illinois at Urbana-Champaign, Urbana, USA.

△ These authors contributed equally to this work.

* E-mail: kschulte@ks.uiuc.edu. Phone: 217-244-1604. Fax: 217-244-6078.

Supporting Material

Text S1: Oseltamivir binds stably to all H5N1 and H1N1pdm wild-type and mutants

The protein root mean squared deviation (RMSD) (Figure S1) of six simulated systems demonstrate that the simulated systems were stable within the timescale simulated. The RMSD of the drug plotted in Figures S2 and S3 over each simulation trajectory, shows that within the first 20 ns equilibrium simulations, the drug bound strongly to wildtype proteins. In mutant systems, drug RMSDs increased after 20ns of simulations. Figure S3, which plots the stability of the drug relative to the active site residues over the entire 40 ns trajectory, reveals movement of the drug that can be traced to fluctuations of its pentyl group (normally bound within a hydrophobic pocket of neuraminidase associated with residues 274 and 294) in the case of H274Y and N294S mutants. These observations support predictions derived from experiments that suggested a role the H274Y and N294S mutations played in disrupting the packing stability of oseltamivir's pentyl group (1). Drug RMSDs were seen to vary in H274Y mutants to a higher degree than that in N294S systems, suggesting that H274Y mutation

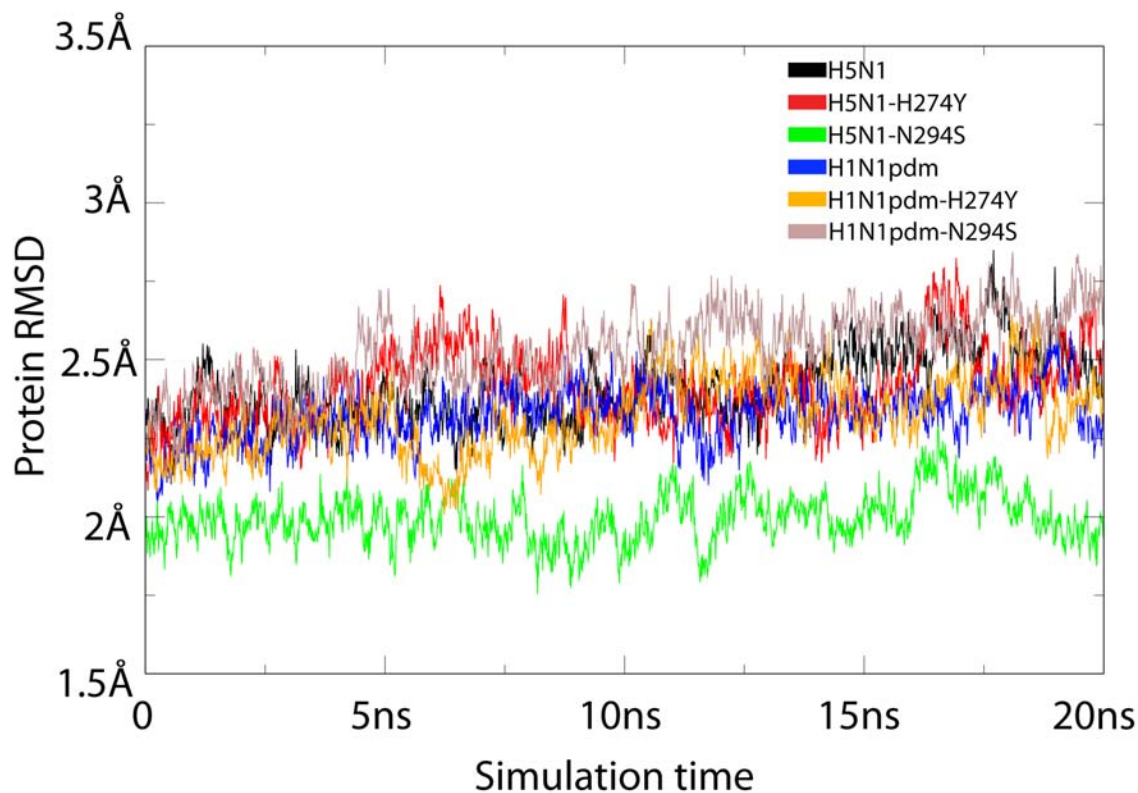


Figure S1: Root mean squared deviation (RMSD) of WT and mutant avian H5N1 and swine H1N1pdm neuraminidases across six 20 ns simulations (*simEQ1* to *simEQ6*). The values reflect the equilibration of each of the neuraminidase systems.

causes a larger disruption of the hydrophobic pocket stabilizing oseltamivir's pentyl group. However, all other critical drug-protein interactions, apart from those with oseltamivir's pentyl group, were observed to be fairly constant with deviations being smallest within the binding pocket; oseltamivir was observed after 40 ns of simulation to remain within the SA active site of all six neuraminidase systems simulated. To investigate if the H274Y and N294S mutations also rupture the hydrogen bonds responsible for stabilizing oseltamivir within the neuraminidase active site, we measured hydrogen bond formation between drug and all wildtype proteins as well as mutants.

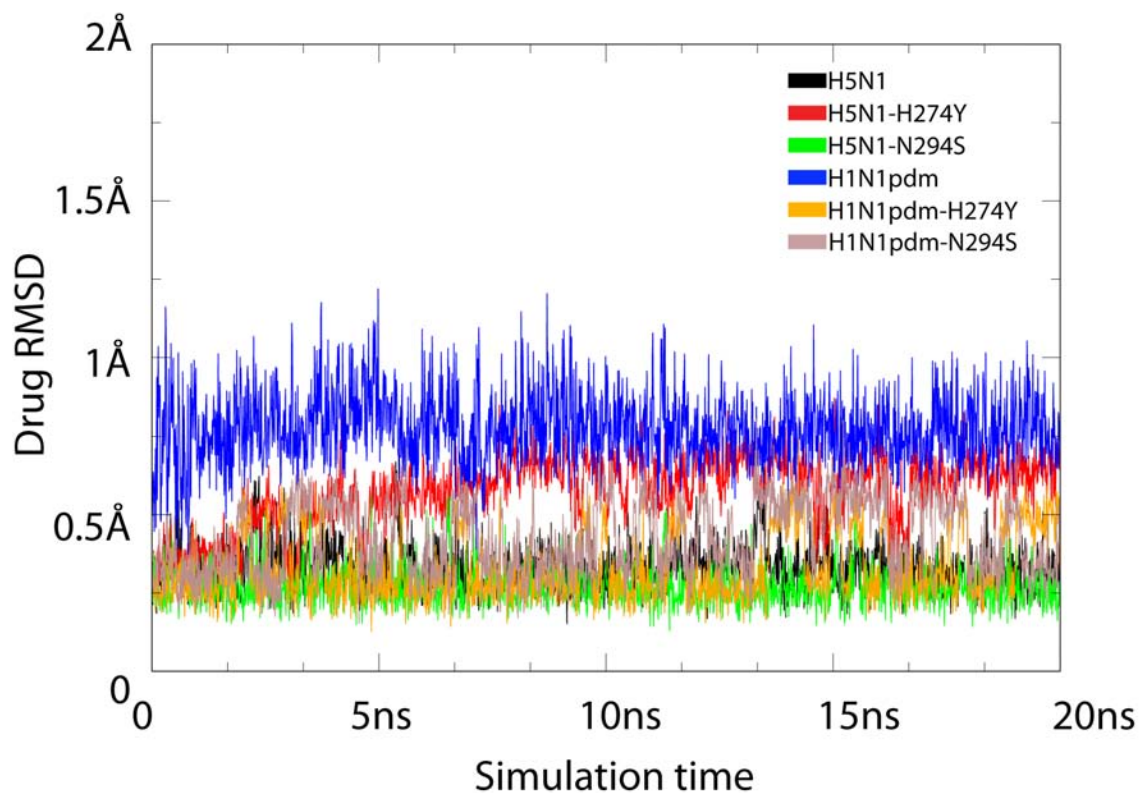


Figure S2: Root mean squared deviation (RMSD) of oseltamivir within the sialic acid (SA) binding pocket of WT and mutant avian H5N1 and swine H1N1pdm, respectively, across six 20 ns simulations (*simEQ1* to *simEQ6* aligned by drug position). The values show that the positions of the drug remain fairly constant with minimal deviation within the binding pocket, thereby permitting the characterization of the specific drug-protein interactions responsible for binding oseltamivir to the active site of neuraminidase N1 subtypes.

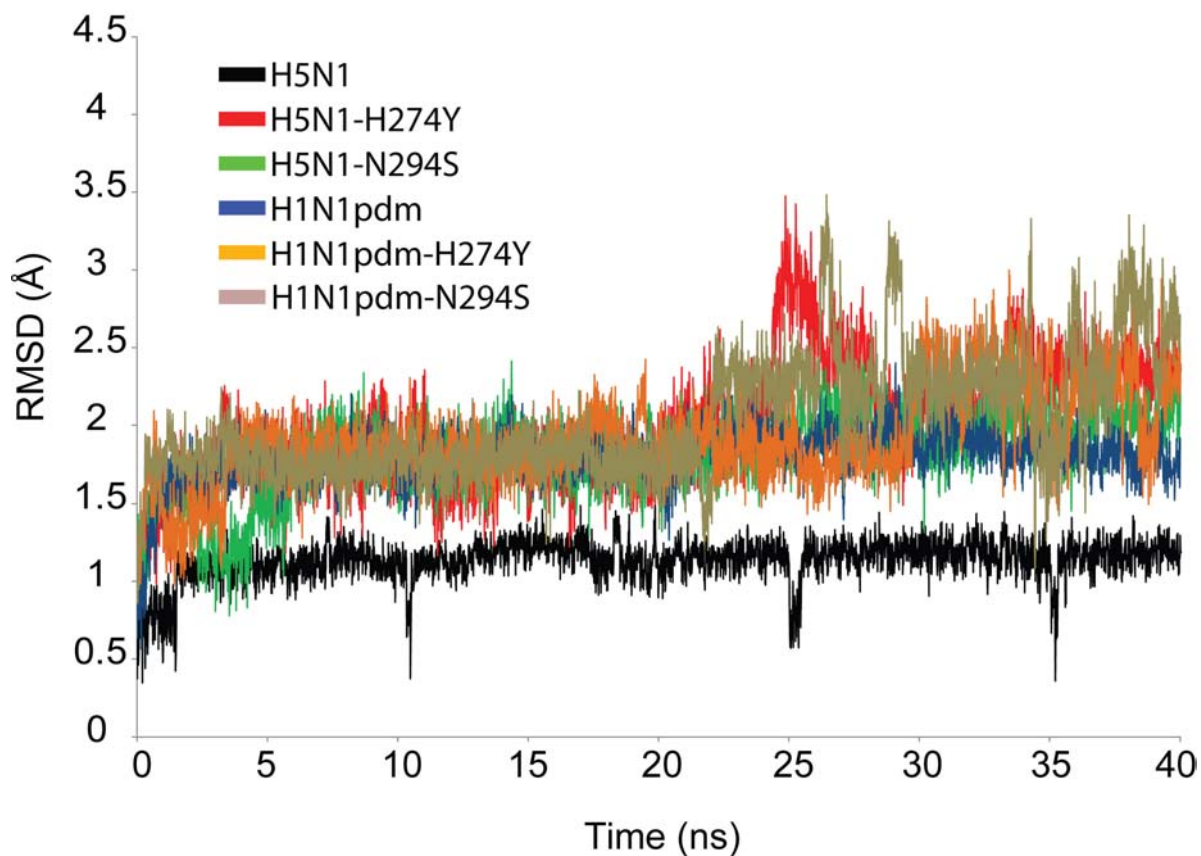


Figure S3: Root mean squared deviation (RMSD) of oseltamivir within the sialic acid (SA) binding pocket of WT and mutant avian H5N1 and swine H1N1pdm, respectively, across six 40 ns simulations (*simEQ1* to *simEQ6* aligned by active site residues). The relative motion of oseltamivir in the mutant systems can be attributed to a rotation of its pentyl group. However, over the entire simulation trajectory the drug remained bound to the neuraminidase active site.

Text S2: Hydrogen bond networks connecting oseltamivir with H5N1 and H1N1pdm neuraminidases

In both wildtype (WT) and mutant simulations, hydrogen bonds between oseltamivir and binding site residues were well conserved, including E119, D151, R292, and R371. Specifically, R292 and R371 were observed to form a hydrogen bond with oseltamivir’s carboxylate moiety, and E119 and D151 with oseltamivir’s amino group. The H274Y mutation, however, appeared to disrupt the hydrogen bonding of oseltamivir’s acetyl group with R152, an interaction which was seen in the wildtype and N294S systems both in *simEQ5* and *simEQ6*. The disruption of the R152 hydrogen bond in the H274Y mutant systems may be attributed to a rotation of oseltamivir’s pentyl group due to disfavorable hydrophobic packing, as discussed below. To the best of our knowledge, the disruption of oseltamivir’s R152 interaction in the H274Y mutant has not been reported in previous studies on the avian H5N1 H274Y mutant (1–3). Results from our respective calculations are presented in Figures S4-A and S5-A, which show histograms of hydrogen bond formation frequency, with schematic views of the specific residues involved in hydrogen bonding in Figures S4-B to D for *simEQ1*, *simEQ3*, and *simEQ5*, respectively, and in Figures S5-B to D for *simEQ2*, *simEQ4*, and *simEQ6*, respectively.

Prior analyses of crystallographic data alone suggested that a hydrogen bond between Y347 and oseltamivir’s carboxyl group, found in the wildtype structure, is lost in the case of the N294S mutant (1), suggesting one possible mechanism of drug resistance. Our simulations produce a dynamic picture of molecular interactions at great resolution that complements the static crystal structure, but do not reveal the presence of a stable hydrogen bond between drug and Y347, not even in the wildtype systems. Prior computational studies of an H5N1+oseltamivir system using the AMBER force field also failed to show evidence that the Y347 hydrogen bond is stable (4). While it is well known that choice of force fields can introduce a bias for protein stability (5), the fact that the Y347 hydrogen bond fails to stay intact for either CHARMM and AMBER force field, supports our conclusion. In our simulations oseltamivir’s carboxyl group was observed to primarily form hydrogen bonds with R292 and R371, having little involvement with Y347. In fact, residue Y347 undergoes rotation to interact strongly with residue W295. Therefore, the suggestion from previous studies on the H5N1 N294S mutant (1; 2), that the N294S mutation in case of H5N1 actually destabilizes hydrogen bonding between oseltamivir and Y347 to induce drug resistance, is not supported by our simulations.

The notable difference between H5N1 and H1N1pdm neuraminidases is the replacement of Y347 by N347 in the drug binding pocket. No conserved drug-protein hydrogen bond was observed for N347 in any of the three H1N1pdm simulations. Given the transient nature of

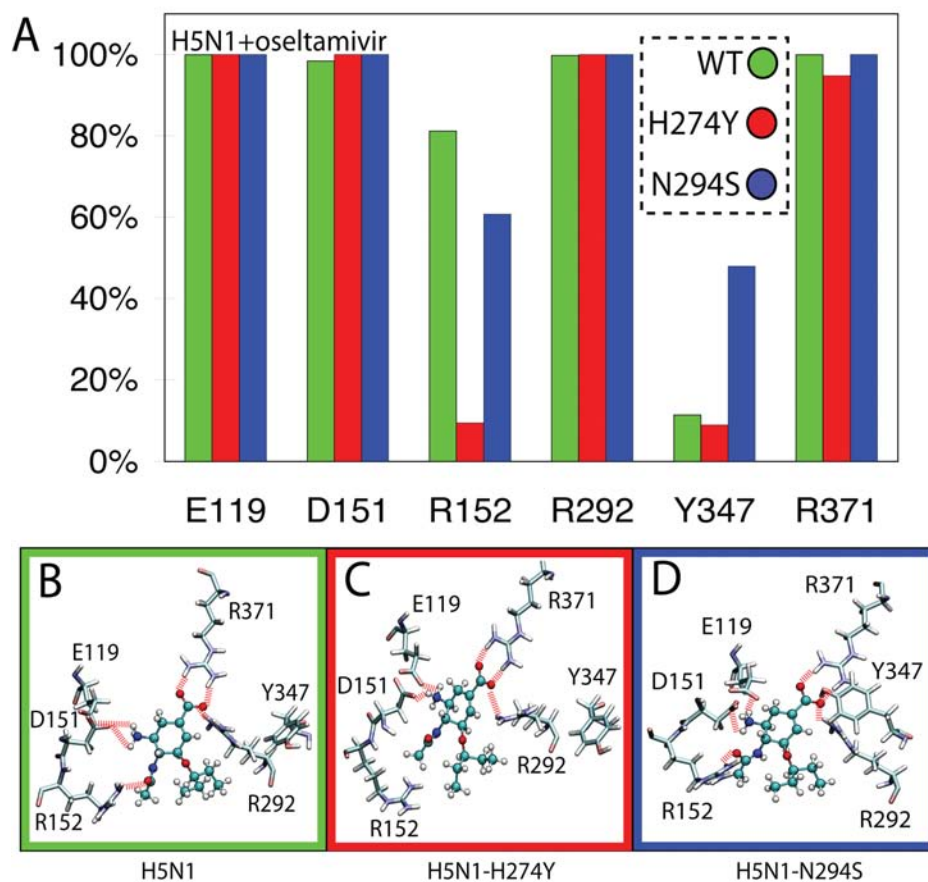


Figure S4: Network and occupancy of hydrogen bonds stabilizing oseltamivir in the SA binding pocket of wildtype and drug-resistant mutant avian H5N1 neuraminidases, in *simEQ1-3*. A) Histograms of hydrogen-bond occupancies for interactions between oseltamivir and residues E119, D151, R152, R292, Y347, and R371 across each simulation run. B) through D) Schematic views depicting the orientation of protein sidechains which form protein-drug hydrogen bonds. Hydrogen bonds in all three simulations were conserved for residues E119, D151, R292, and R371. The H274Y mutation was observed to disrupt hydrogen bonding to R152. Despite the increased interaction with Y347 in the case of the N294S mutant, the hydrogen bonds between oseltamivir and Y347 were not stable in any of the simulated systems.

even the N294S mutant induced hydrogen bond involving residue 347 in the case of H5N1, and the lack of interaction with residue 347 in any of the other simulations, it is highly unlikely that the single residue change (Y347 to N347), between the H5N1 and H1N1pdm strains, significantly alters the drug-protein stability in regard to the hydrogen bond network involved.

Text S3: H274Y mutation disrupts hydrophobic packing of oseltamivir’s pentyl group in both H5N1 and H1N1pdm neuraminidase

Beside disrupting the drug-protein hydrogen-bonding network, the N274Y mutation may induce drug resistance by disrupting the hydrophobic packing of the drug into the protein binding pocket. Through inspection of the static crystal structures of the H274Y and N294S mutants of H5N1, it has been suggested that the mutations disrupt favorable hydrophobic packing interactions necessary for strong binding of oseltamivir (1). In our simulations of WT H5H1 and H1N1pdm, the packing of oseltamivir’s pentyl moiety tends to favor close association with residues I222, R224, A246, and E276. To test the effect of mutations H274Y and N294S on hydrophobic interactions of oseltamivir’s pentyl group with the proteins, we monitored the solvent accessible surface area (SASA) of oseltamivir’s pentyl group for all simulation trajectories. While there was no significant change to the pentyl group SASA (henceforth referred to as PG-SASA) in the wildtype and N294S mutant for either H5N1 or H1N1pdm neuraminidases, an outward rotation of the pentyl group was observed for H274Y, discernable in oseltamivir’s binding pose and evident in a notably higher calculated PG-SASA. The PG-SASAs for all simulated systems are shown in Figure S6, with inset images of oseltamivir’s binding pose in simH1N1pdm (Figure S5A) and simH1N1pdm-H274Y (Figure S6B), illustrating the rotation of the pentyl group towards the open mouth of the binding pocket.

Previously published MD simulations performed over relatively short time scales (3 to 6 ns) have suggested two possible mechanisms: 1) that the H247Y mutation reduces the size of the hydrophobic pocket within the SA binding pocket near oseltamivir’s pentyl moiety (3) and 2) that the H274Y mutation breaks a critical salt bridge between E276 and R224 to disrupt drug binding (2). Our longer (40ns) simulations were able to corroborate mechanism 1 (as shown by the increase in PG-SASA in the case of the H274Y mutant simulations), but not mechanism 2. In fact, in all six of our simulations, E276 maintains stable charge-charge interactions (salt bridging) with R224 despite displacement of the drug from the protein I222-R224-A246-E276 pocket in the case of H274Y mutants. This drug displacement increases water penetration into the pocket (Figure S6). Our simulations support therefore predictions

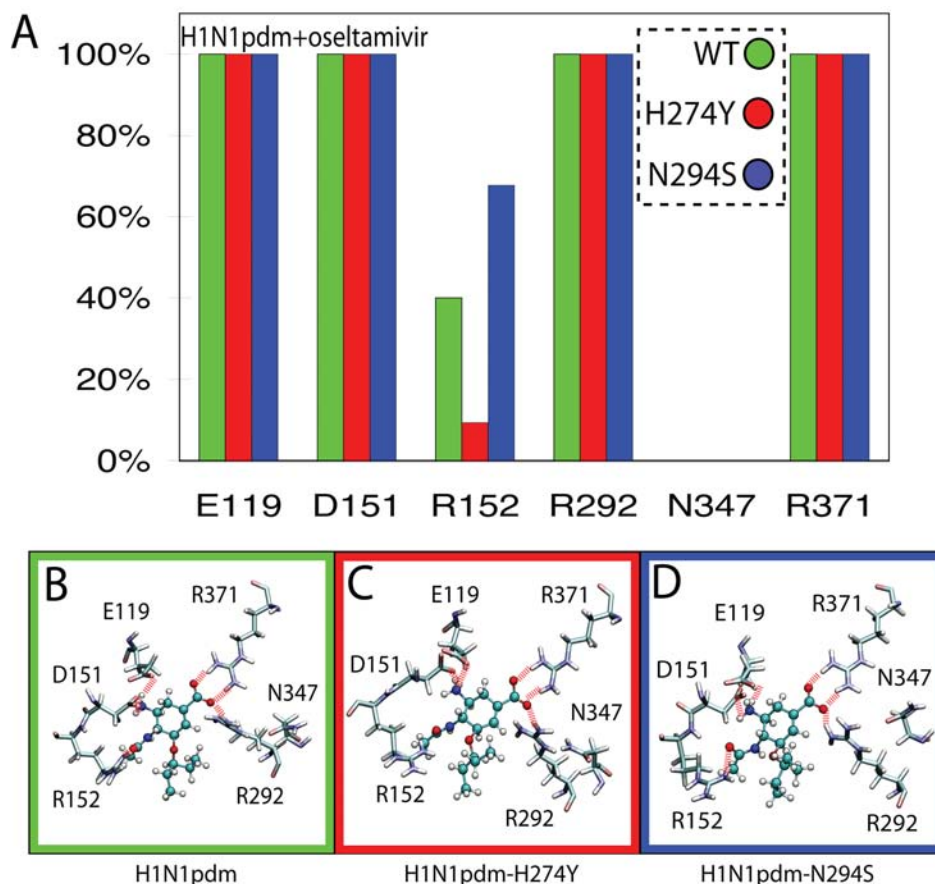


Figure S5: Network and occupancy of hydrogen bonds stabilizing oseltamivir in the SA binding pocket of wildtype and drug-resistant mutant avian H1N1pdm neuraminidases, in *simEQ4-6*. A) Histograms of hydrogen-bond occupancies for interactions between oseltamivir and residues E119, D151, R152, R292, N347, and R371 across each simulation run. B) through D) Schematic views depicting the orientation of protein sidechains which form protein-drug hydrogen bonds. Hydrogen bonds in all three simulations were conserved for residues E119, D151, R292, and R371. The H274Y mutation was observed to disrupt hydrogen bonding to R152. Interestingly, residue 347, which distinguishes the binding pocket of H1N1pdm from H5N1, makes no contribution to the drug-protein hydrogen-bond network in the case of H1N1pdm.

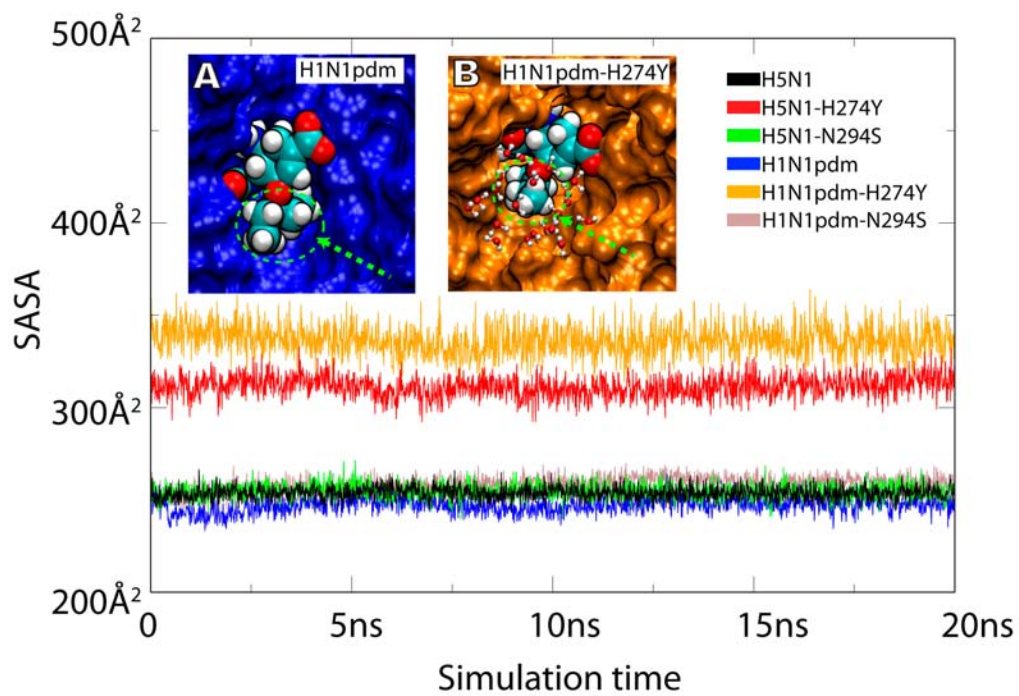


Figure S6: Solvent accessible surface area of oseltamivir's pentyl group (PG-SASA) in simulations of H5N1 and H1N1pdm WT and mutants.

from earlier studies of a possible mechanism for the H274Y mutation-induced drug resistance through water infiltration and destabilization of favorable drug packing (1).

Text S4: Orientation of loops 150 and 430 in relation to the charged binding funnel.

The electrostatic potential of N1 neuraminidase (as discussed in the main text) revealed a novel charged binding funnel which may direct the passage of oseltamivir. In previous studies, two flexible loops (150 and 430) at the periphery of the binding pocket appeared to play an important role in ligand binding (6; 7). The positions of these loops, though, are located sufficiently distant from the novel charged binding funnel such that they quite apparently do not function as gating elements for this particular pathway. This is illustrated in Figure S7.

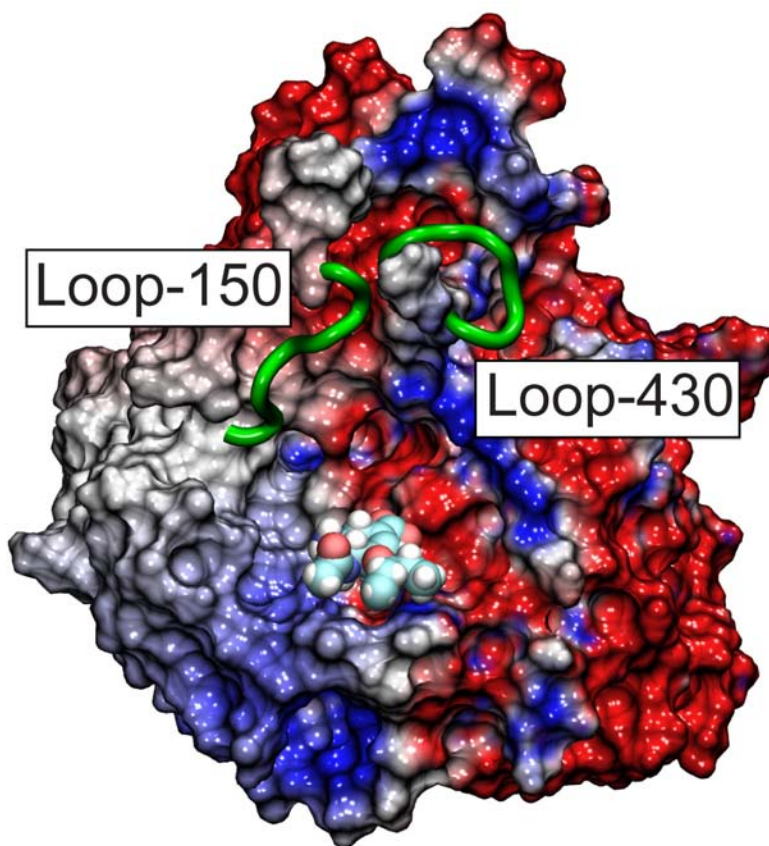


Figure S7: The position of flexible loops 150 and 430 relative to the charged binding funnel of H5N1 neuraminidase.

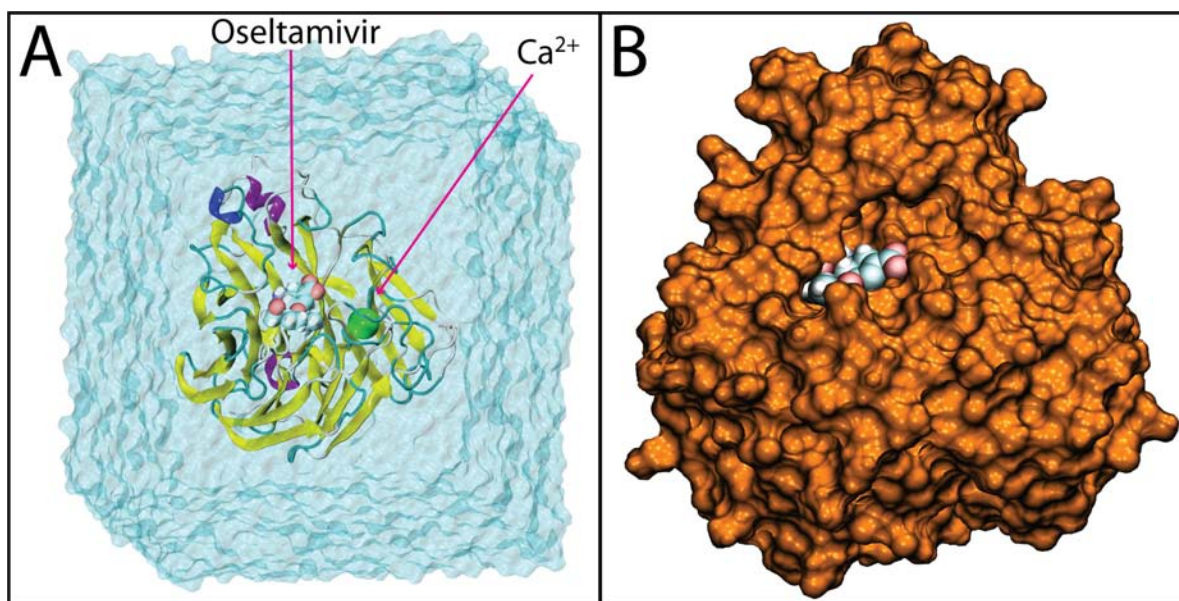


Figure S8: Drug bound systems simulated. Shown here is a representative example of H1N1pdm bound to oseltamivir. In A), the system is shown in the solvation box and with oseltamivir and the active site calcium ion. In B), oseltamivir is shown buried in the SA binding pocket of H1N1pdm, the latter rendered in surface view.

Videos

Video S1. (S1.avi) Trajectory from *simSMD1*, where a force is applied to oseltamivir perpendicular to the plane of the SA binding pocket. Despite the direction of force, oseltamivir interacts with and follows the charged electrostatic pathway identified and discussed in Figure 1, with snapshots shown in Figure 3.

Videos S2-S4. (S2, S3, and S4.avi) Videos S2-S4 depict trajectories from *simFEQ1-3*, respectively showing the spontaneous diffusion of oseltamivir out of the neuraminidase binding pocket via interaction with the electrostatic binding funnel (see Figure 3 for snapshots from *simFEQ1*).

Video S5. (S5.avi) Video S5 depicts the trajectory from *simFEQ4*, where oseltamivir briefly interacts with the electrostatic binding funnel before diffusing out of the neuraminidase binding pocket via an alternate pathway in the region of the “430-loop” (8) shown in green

in Figure 3.

Video S6. (S6.avi) Video S6 depicts the trajectory from *simFEQ5*, where oseltamivir diffuses out of the neuraminidase active site via interaction with the electrostatic binding funnel, fails to enter the active site at a different location on the periphery of the binding pocket due to electrostatic repulsion, and then rebinds stably to neuraminidase through the electrostatic binding funnel. See Figure 6 for snapshots.

Videos are also provided in Quicktime (.mov) format for compatibility with Apple/Mac software.

References

1. Collins, P. J., L. F. Haire, Y. P. Lin, J. Liu, R. J. Russell, P. A. Walker, J. J. Skehel, S. R. Martin, A. J. Hay, and S. J. Gamblin. 2008. Crystal structures of oseltamivir-resistant influenza virus neuraminidase mutants. *Nature*. 453:1258–1261.
2. Nick, X. W. and J. J. Zheng. 2009. Computational studies of H5N1 influenza virus resistance to oseltamivir. *Prot. Sci.* 18:707–715.
3. Malaisree, M., T. Rungrotmongkol, N. Nunthaboot, O. Aruksakunwong, P. Intharathep, P. Decha, P. Sompornpisut, and S. Hannongbua. 2009. Source of oseltamivir resistance in avian influenza H5N1 virus with the h274y mutation. *Amino Acid*. 37:725–732.
4. Malaisree, M., T. Rungrotmongkol, P. Decha, P. Intharathep, O. Aruksakunwong, and S. Hannongbua. 2008. Understanding of known drug-target interactions in the catalytic pocket of neuraminidase subtype N1. *Proteins: Struct., Func., Bioinf.* 71:1908–1918.
5. Freddolino, P. L., S. Park, B. Roux, and K. Schulten. 2009. Force field bias in protein folding simulations. *Biophys. J.* 96:3772–3780.
6. Amaro, R. E., D. D. L. Minh, L. S. Cheng, J. A. J. O. William M. Lindstrom, J.-H. Lin, and W. W. L. J. A. McCammon. 2007. Remarkable loop flexibility in avian influenza N1 and its implications for antiviral drug design. *J. Am. Chem. Soc.* 129:7764–7765.
7. Amaro, R. E., X. Cheng, I. Ivanov, D. Xu, and J. A. McCammon. 2009. Characterizing loop dynamics and ligand recognition in human- and avian-type influenza neuraminidases via generalized born molecular dynamics and end-point free energy calculations. *J. Am. Chem. Soc.* 131:4702–4709.
8. Cheng, L. S., R. E. Amaro, D. Xu, W. W. Li, P. W. Arzberger, and J. A. McCammon. 2008. Ensemble-based virtual screening reveals potential novel antiviral compounds for avian influenza neuraminidase. *J. Med. Chem.* 51:3878–3894.